Chapter 4

Contraction by Ca^{2+} Influx via the L-Type Ca^{2+} Channel Voltage Window in Mouse Aortic Segments is Modulated by Nitric Oxide

Paul Fransen, Cor E. Van Hove, Johanna van Langen and Hidde Bult

Additional information is available at the end of the chapter

http://dx.doi.org/10.5772/47771

1. Introduction

L-type Ca^{2+} channels play a dominant role in blood pressure regulation as suggested by the fall in mean arterial blood pressure in mice with selective ablation of the channel gene (CACN1C) in vascular smooth muscle cells (VSMCs) (Moosmang et al., 2003), the increased CACN1C gene expression in VSMCs in rodent models of hypertension (Pesic et al., 2004; Rhee et al., 2009), the anti-hypertensive effect of L-type Ca^{2+} channel blockers (CaBs) (Mancia et al., 2007) and the relationship between an autoantibody against vascular L-type Ca^{2+} channels and clinical characteristics of hypertensive patients (Zhou et al., 2008). Transcripts and protein expression of CACN1C are found widely in the cardiovascular system, where the ion channels serve the time- and voltage-dependent influx of Ca^{2+} ions to initiate muscle contraction (Akata, 2007; Bers, 2002). It is now recognized, however, that not only peripheral resistance but also arterial compliance is of great importance, especially in old age (systolic) hypertension (Belz, 1995; Mitchell, 1999; Westerhof et al., 2009). In the large conduit arteries, L-type Ca^{2+} channels are important determinants of their mechanical properties and compliance, which are such that blood pressure and flow are propagated between the heart and arterioles and that thereby pulsatile flow is transformed into steady flow due to the "windkessel" effect (Westerhof et al., 2009). For example, CaBs increase vascular compliance of large elastic vessels and may be of importance for the pathogenesis and prognosis of cardiovascular complications such as atherosclerosis, left ventricular hypertrophy and heart failure (Bellien et al., 2010; Belz, 1995; Essalihi et al., 2007; Safar et al., 1989; Slama et al., 1995; Vayssettes-Courchay et al., 2011). Further evidence for a role of L-type Ca^{2+} channels in atherosclerosis was obtained in carotid and femoral VSMCs, where the L-type Ca^{2+} channel gene expression differs between atherosclerotic versus non-atherosclerotic regions (Tiwari et al., 2006). Not only Ca^{2+} channels but also endothelial released nitric oxide

(NO) may be involved in these processes. Inhibition of endothelial NO synthase (eNOS) with N^{Ω}-nitro-L-arginine methyl ester (L-NAME) or N^{Ω}-nitro-L-arginine (L-NNA) causes hypertension and the decrease of basal endothelial NO release or availability may be at the basis of increased reactivity to vasoconstrictors in hypertension (Panza et al., 1993). Furthermore, in the beginning of plaque development in animal models and in patients with atherosclerotic symptoms or risk factors, eNOS activity and concomitant NO release is altered, especially in atherosclerosis-prone aortic segments (Fransen et al., 2008; Kauser et al., 2000; Vanhoutte et al., 2009). Recently, we showed that L-type Ca^{2+} influx and its inhibition with CaBs may also have consequences for the capacity of NO to relax constricted mouse aorta. The relaxing efficacy of NO in mouse aorta was dependent on the contractile agonist, and more specifically, decreased when the contraction was mainly elicited via L-type Ca^{2+} influx, but increased when Ca^{2+} influx was partially inhibited with CaBs (Van Hove et al., 2009). The above observations may suggest an interaction between basal NO and VSMC L-type Ca^{2+} channels. An inhibitory effect of NO on Ca^{2+} currents in vascular smooth muscle and cardiomyocytes has been described (Blatter & Wier, 1994; Fischmeister et al., 2005; Tsai & Kass, 2009), but has not been associated with L-type Ca^{2+} channel-mediated contractions in mouse aorta. This chapter will focus on the specific role of L-type Ca^{2+} channels in vasoconstriction and dilation and the interplay between NO and these L-type Ca^{2+} channels.

2. Interaction between endothelial and vascular smooth muscle cells in intact mouse aorta

It is generally assumed that the increase of intracellular Ca^{2+} in vascular endothelial cells results in release of NO via complex interactions with calmodulin, caveolin, endothelial NOS (eNOS) and tetrahydrobiopterin. NO released from the endothelial cells stimulates guanylate cyclase (sGC) to produce cGMP, which causes relaxation of the VSMCs via reduction of intracellular Ca^{2+} and the Ca^{2+}-sensitivity of the contractile elements. Reduction of intracellular Ca^{2+} can occur via different mechanisms: inhibition of IP_3-mediated Ca^{2+} release from intracellular Ca^{2+} stores; removal and sequestration of intracellular Ca^{2+} pump mechanisms and/or both direct and indirect inhibition of influx of extracellular Ca^{2+} through voltage-gated Ca^{2+} channels (Tsai & Kass., 2009). In baseline conditions, i.e. in the absence of receptor-stimulation with agonists such as acetylcholine (ACh), there is basal release of NO through constitutive activity of endothelial eNOS in the mouse aorta. In isolated arteries, the basal NO production can be assessed by comparing force development by the SMCs in response to a vasoconstrictor such as phenylephrine in the absence and presence of NOS inhibitors. On the other hand, receptor-stimulated eNOS activity can be determined based on its sensitivity for agonists like ACh to induce endothelium-dependent relaxation of preconstricted segments. Remarkably, basal and stimulated eNOS activity are differentially regulated. In rat aorta, basal NO release is more sensitive to destruction by superoxide anion, and can be selectively inhibited by N^{Ω}-monomethyl-L-arginine (L-NMMA) and asymmetric N^{Ω}-dimethyl-L-arginine (ADMA) without ACh responses being affected (Al-Zobaidy et al., 2011; Frew et al., 1993; Mian & Martin, 1995).

Differences between basal and stimulated eNOS activity were also observed in apolipoprotein E-deficient (apoE$^{-/-}$) mice which develop atherosclerotic lesions in the thoracic aorta spontaneously at the age of 6 months, a process, which can be effectively accelerated by feeding these mice a high cholesterol diet. The mice exhibit preferential lesion formation in the aortic root and arch, and the proximal and distal part of the thoracic aorta (Crauwels et al., 2003; Nakashima et al., 1998; Reddick et al., 1994). This makes the apoE$^{-/-}$ mouse an interesting model to study differences between atherosclerosis-prone and atherosclerosis-resistant regions. We have previously shown that at the age of 4 months, hence, before development of any visible lesions in the apoE$^{-/-}$ mouse model, basal and agonist-stimulated NO release decreased, respectively increased in atherosclerosis-prone aortic segments of apoE$^{-/-}$ in comparison with wild-type (WT) mice (Fransen et al., 2008). Because no differences in eNOS expression were found between aorta of WT and apoE$^{-/-}$ mice, this indicated that the release or efficacy of NO differed between both mouse strains. In non-stimulated conditions the compromised basal NO release in the apoE$^{-/-}$ mouse might be related to lower intra-endothelial Ca^{2+} concentrations because it could be restored to "normal" wild-type levels by experimentally increasing intracellular Ca^{2+}. Agonist (ACh)-stimulated VSMC relaxation was temporally and dose-dependently related to the increase of endothelial Ca^{2+}. Although the agonist-stimulated increase of endothelial Ca^{2+} was similar in both strains, apoE$^{-/-}$ segments were significantly more sensitive than WT segments in their relaxation to ACh. Results of these studies might suggest an important role of basal and stimulated eNOS activity in the pathophysiology of atherosclerotic lesions.

In functional and molecular biological studies we have further demonstrated that before development of any visible lesions, not only endothelial cells but also the SMCs of the thoracic aorta of apoE$^{-/-}$ mice displayed altered intracellular Ca^{2+} homeostasis in comparison with WT VSMCs (Van Assche et al., 2007) and that within the apoE$^{-/-}$ strain the smooth muscle transcriptome is altered at atherosclerosis-prone versus atherosclerosis-resistant locations (Van Assche et al., 2011). Hence, not only endothelial, but also VSMC function is altered in atherosclerosis-prone versus -resistant segments. Whether the cross-talk between both cell types is affected in both directions during the process of atherosclerosis, is far less studied. At least, we have shown before that NO-dependent vasodilation is dependent on the agonist causing contraction and whenever VSMC function alters during development of atherosclerosis, this is also expected to affect the efficacy of endothelial cell stimulation.

3. Relaxation of VSMCs depends on the agonist causing contraction

Contractions of isolated arteries are often studied by initiating VSMC intracellular Ca^{2+} increase with two widely used and different stimuli. On the one hand, elevated external K^+ depolarises the VSMCs and elicits multiphasic Ca^{2+} signalling and force development through influx of extracellular Ca^{2+} via L-type Ca^{2+} channels. On the other hand, α_1-adrenoceptor stimulation with phenylephrine also causes multiphasic Ca^{2+} signalling and force development, but the signalling is different from the depolarization-induced signalling. The vasodilator effects of NO differ significantly for both contractile agents. Bigger contractions produced by increasing concentrations of phenylephrine were all

equally sensitive to relaxation by ACh (figure 1) or the NO donor DEANO. In contrast, when the VSMCs were clamped to depolarized membrane potential (V_m) with high extracellular K^+ concentrations, relaxation by ACh or DEANO became attenuated as K^+-induced force augmented (figure 1) (Van Hove et al., 2009).

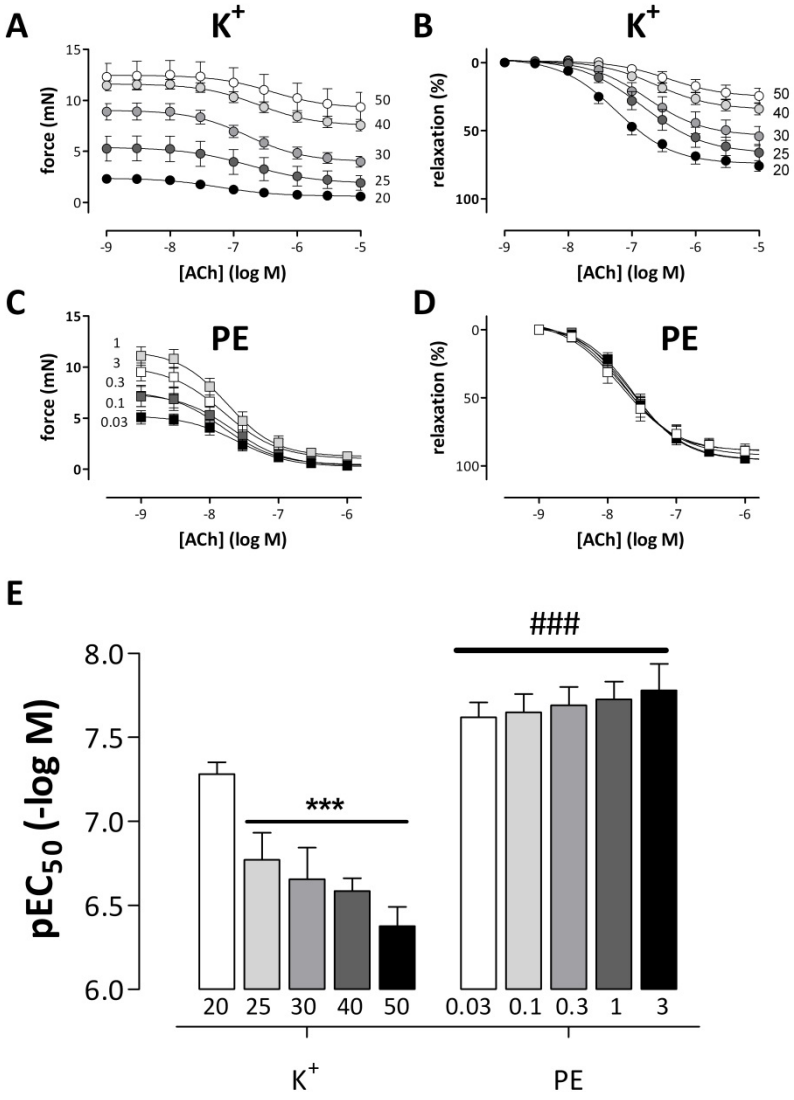

Figure 1. Relaxation induced by ACh-stimulation of mouse aortic segments at different levels of contraction induced by depolarization (K^+) or phenylephrine (PE). A, C: absolute values; B, D: normalized values. Relaxation curves were fitted with sigmoidal concentration-response equations with variable slope, which revealed maximal responses (E_{max}) and the negative logarithm of the concentration resulting in 50% of the maximal effect (pEC_{50}). Relaxation curves after contraction by increasing depolariza-

tion were shifted to the right as external K^+ concentration (and force level, A) increased. Not only the maximal amplitude produced by ACh declined significantly, but also the $logEC_{50}$ of ACh was significantly shifted to the right (E). In contrast, the normalized relaxation curves after contraction elicited by increasing phenylephrine concentrations were identical at each contraction level, and there was only a minor shift of the $logEC_{50}$ (E). ***: P< 0.001 versus 20 mM K^+ ###: P<0.001 versus K^+; n=5; mean±SEM. Modified after figure 2 in (Van Hove et al., 2009)

Simultaneous measurement of intracellular Ca^{2+} and force development in SMCs of de-endothelialised aortic segments revealed important differences between Ca^{2+} signals in depolarization (50 mM K^+)- or phenylephrine-constricted segments upon addition of DEANO, a donor of exogenous NO (figure 2). For phenylephrine-induced contractions and

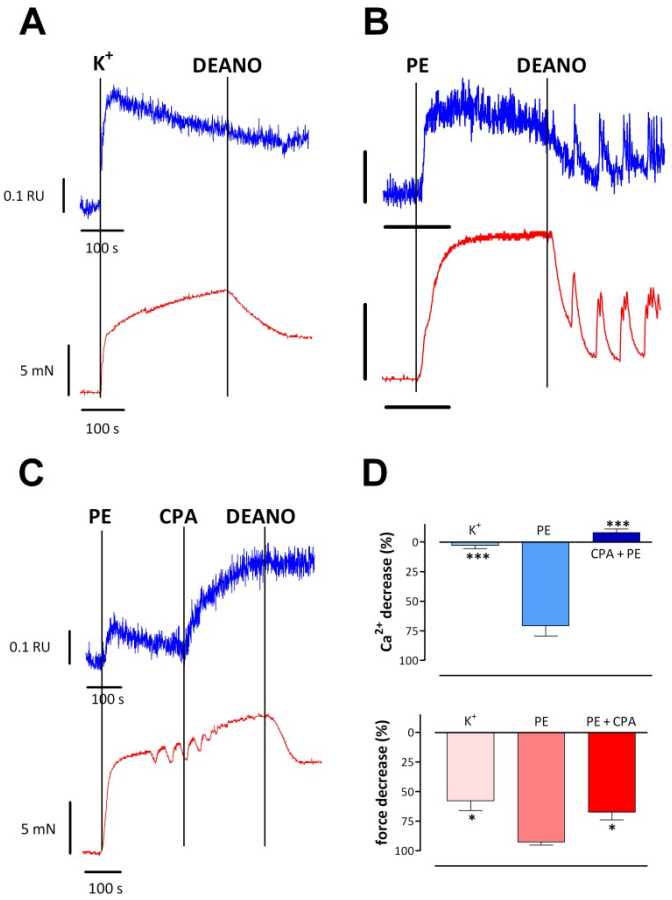

Figure 2. Mobilisation of intra-VSMC Ca^{2+} (Fura-2 technique) and concomitant isometric force before and after addition of 10 μM DEANO to 50 mM K^+ (A) and 3 μM phenylephrine (PE) in the absence (B) and presence of 10 μM cyclopiazonic acid (CPA, C). D shows the mean±SEM of Ca^{2+} and force decrease after addition of DEANO. Data in D: mean±SEM, n=4 endothelium-denuded segments; *, ***: P<0.05, 0.001 versus phenylephrine. Modified after figure 6 in (Van Hove et al., 2009).

VSMC Ca^{2+} signals, addition of NO resulted in an abrupt decrease of intracellular Ca^{2+}, which could be blocked by adding cyclopiazonic acid (CPA), an inhibitor of the sarcoplasmic reticulum (SR) Ca^{2+} pump (SERCA), but not by inhibition of sGC with 1H-[1,2,4]oxadiazolo[4,3-a]quinoxalin-1-one (ODQ). Results indicated a direct stimulation by NO of Ca^{2+} re-uptake to the SR by SERCA, which is in accordance with previous reports (Cohen et al., 1999; Cohen & Adachi, 2006; Van Hove et al., 2009). Contractions, but not Ca^{2+} signals of VSMCs, depolarized with 50 mM K^+, declined upon addition of exogenous NO. Nevertheless, as seen for contractions by depolarization with elevated K^+, also phenylephrine-induced contractions are associated with depolarization and opening of L-type Ca^{2+} channels (Akata, 2007; Plane et al., 1998; Quignard et al., 2000; Richards et al., 2001; Van Hove et al., 2009). If L-type Ca^{2+} influx is an important determinant of the vasodilator capacity of NO, why then is there an abrupt decrease of intracellular Ca^{2+} in the VSMCs after addition of exogenous NO to phenylephrine-elicited contractions and not to 50 mM K^+-evoked contractions? Reduction of Ca^{2+} influx in depolarized segments with CaBs increased NO´s capacity to dilate the segments, indicating that not only the depolarized V_m of the VSMCs, but also the amount of Ca^{2+} influx determines the efficacy of NO to cause complete relaxation (Van Hove et al., 2009). Therefore, it was decided to investigate the phenylephrine- and K^+-induced isometric contractions in more detail.

4. Phenylephrine-induced contractions and NO

Addition of phenylephrine causes intracellular Ca^{2+} release from intracellular SR Ca^{2+} stores via activation of IP_3-receptors (Karaki et al., 1997). Indeed, in the absence of extracellular Ca^{2+} phenylephrine causes emptying of the SR Ca^{2+} stores and elicits a transient contraction (figure 3). This transient contraction in Ca^{2+}-free conditions is higher with the constitutive activity of eNOS because inhibition of basal NO release decreased the IP_3-mediated contraction by phenylephrine (figure 3). These results are compatible with previous observations that basal NO stimulates SERCA activity (Cohen et al., 1999; Cohen & Adachi., 2006; Van Hove et al., 2009). Thereby, the Ca^{2+} content of the SR stores of the VSMCs may be increased and may then lead to higher IP_3-mediated contractions. The transient contractions by phenylephrine in the absence of extracellular Ca^{2+} were dose-dependently inhibited by exogenous NO (DEANO, figures 4A, B). This suggests that although basal NO might stimulate Ca^{2+} uptake to the SR via stimulation of SERCA, it inhibits the IP_3-mediated release of Ca^{2+} or the concomitant transient contraction. When these experiments were repeated with addition of ACh to promote endothelial NO release, however, relaxation of phenylephrine-induced contractions by increasing concentrations of ACh in the absence of external Ca^{2+} was completely absent (figures 4C, D). These experiments demonstrate the absolute necessity of external Ca^{2+} to induce ACh-stimulated release of NO from the endothelial cells. Although ACh has been described to release Ca^{2+} from the SR (Fransen et al., 1998), this release does not stimulate eNOS to inhibit IP_3-mediated contractions in mouse aortic SMCs. Hence, release of endogenous NO is dependent upon influx of extracellular Ca^{2+} into the endothelial cells. It has been observed before that Ca^{2+} influx into the endothelial cells stimulated NO production more potently than Ca^{2+} released from internal stores, which evokes little NO

production (Isshiki et al., 2002; Isshiki et al., 2004). This is also consistent with old observations that the resting level of cGMP falls after removal of external Ca^{2+} (White & Martin, 1989). In other studies, it has been shown that the TRPV4-mediated Ca^{2+} signal was required for eNOS activation by ACh (Adapala et al., 2011; Zhang et al., 2009), also illustrating the necessity of Ca^{2+} influx for endothelial NO release. Isshiki et al. (Isshiki et al., 2004) suggested that agonist-stimulated eNOS activity in the endothelial cells was sensitive to external Ca^{2+}-dependent acute changes in intracellular subcortical Ca^{2+} signals and that basal eNOS activity was maintained and regulated by subplasmalemmal Ca^{2+} equilibrated with extracellular Ca^{2+}.

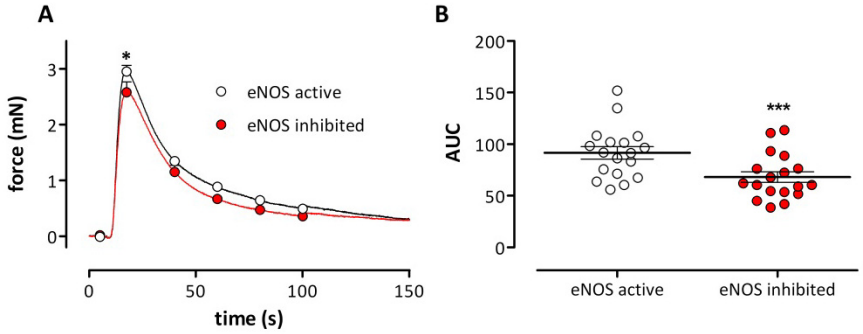

Figure 3. Effect of basal NO release on transient contractions by phenylephrine in the absence of external Ca^{2+}. A: IP_3-mediated contractions by 2 μM phenylephrine in the absence of extracellular Ca^{2+} (0 mM Ca^{2+} + 2 mM EGTA) before (black, open symbol) and after inhibition (red, closed symbol) basal eNOS activity with 300 μM LNAME/LNNA. In B the area under the curve (AUC) shows that the transient contraction is significantly larger with eNOS active than with eNOS inhibited. (A: mean contraction (n=18) with mean force value±SEM at certain time points).

Concomitant with the transient contraction, due to IP_3-mediated Ca^{2+} release, α_1-adrenoceptor stimulation with phenylephrine causes also tonic contractions, which are measureable only in the presence of external Ca^{2+} (figure 5A). These contractions are mediated by Ca^{2+} influx from the extracellular medium via Ca^{2+}-permeable channels (SOCE or store-operated Ca^{2+}-entry). The Ca^{2+} entry occurs via L-type Ca^{2+} channels, which can be inhibited with CaBs (figure 5B) and via non-selective cation channels, which can be inhibited with 50 μM 2-aminoethoxydiphenylborane (2-APB) (Bootman et al., 2002; Peppiatt et al., 2003) (figure 5C). Addition of verapamil (CaB) or 2-APB between the phasic and tonic contraction (figure 5B, C) results in reduced SOCE and SOCE-related contraction. The SOCE contraction in the presence of 2-APB can be completely inhibited with CaBs, indicating it is mediated by L-type Ca^{2+} influx only, whereas the SOCE contraction in the presence of verapamil can be completely inhibited with 2-APB, indicating it is mediated by non-selective cation Ca^{2+} influx only. Figure 6 compares relaxation by ACh of phenylephrine-preconstricted aortic segments in control conditions (contractions in the presence of external Ca^{2+}), upon re-addition of external Ca^{2+} (SOCE contractions) and following inhibition of the cation channel-mediated Ca^{2+} influx with 2-APB.

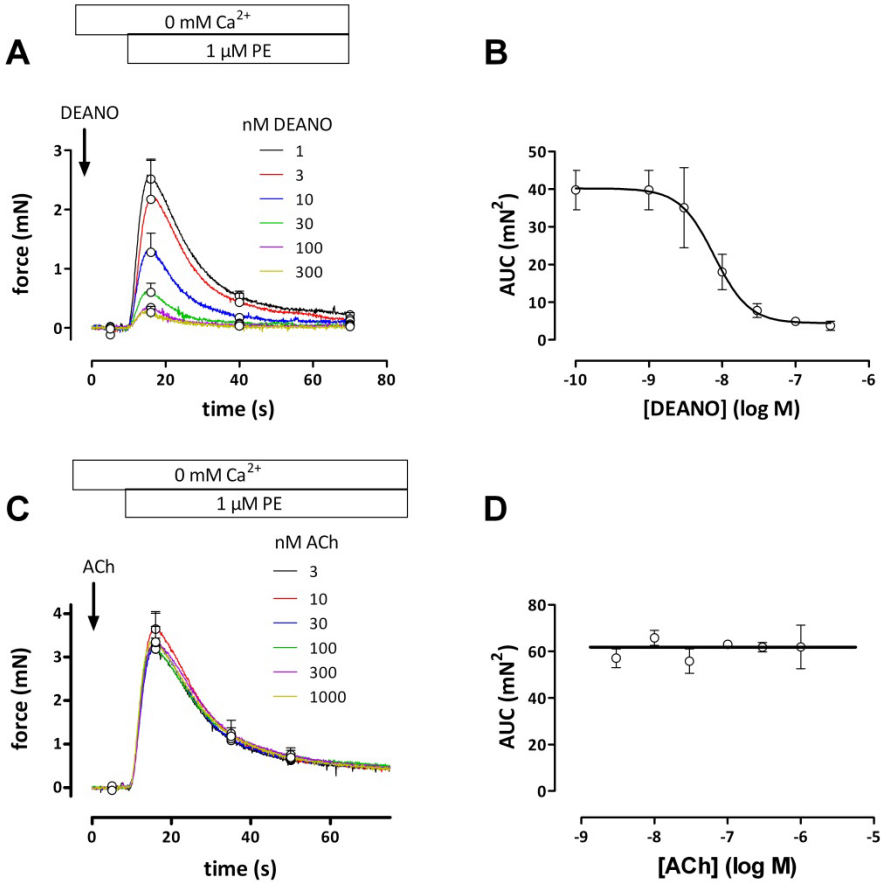

Figure 4. Exogenous NO, but not ACh inhibits IP_3-mediated contraction evoked by 1 µM phenylephrine in the absence of external Ca^{2+}. A: Force development by 1 µM phenylephrine (PE) after eNOS inhibition with 300 µM LNAME/LNNA. Force was measured 3 minutes after switching to 0 mM Ca^{2+}. Before the transient contraction increasing concentrations of DEANO (indicated in nM) were applied. B: Dose-effect relationship for the inhibition by DEANO of the area under the curve (AUC) for the different IP_3-mediated phenylephrine-elicited contractions. C: IP_3-mediated phenylephrine-elicited contractions in segments with eNOS active were not influenced by increasing concentrations of ACh (indicated in nM). D: Dose-effect relationship for the inhibition by ACh of the AUC for the IP3-mediated phenylephrine-elicited contractions. $LogEC_{50}$ for DEANO was -8.12±0.20 logM. Data: mean±SEM at certain time points; n= 4.

Relaxation by ACh of these tonic phenylephrine-induced contractions were not different for control contractions (normal Krebs-Ringer solution with external Ca^{2+}) or SOCE contractions (elicited by re-addition of external Ca^{2+} after emptying the stores with phenylephrine) (figure 6A). When Ca^{2+} influx via non-selective cation channels during the phenylephrine-induced SOCE contraction was inhibited with 2-APB, the tonic contraction induced by phenylephrine was significantly smaller and relaxation by ACh was reduced by about 50%

(figure 6B). Results indicate that the relaxing capacity of NO is small when contractions are mediated by Ca^{2+} influx via L-type Ca^{2+} channels as shown before for depolarization-mediated contractions. These results further confirmed the hypothesis that the difference in NO-mediated relaxation of segments depolarized with K^+ versus phenylephrine, as shown in figure 1, is due to the amount of Ca^{2+} influx via L-type Ca^{2+} channels and the membrane potential (V_m) of the VSMCs. Whereas relaxation of contractions elicited with high external K^+ was not complete, was not associated with re-uptake of Ca^{2+} to the SR or with a significant decrease of intracellular Ca^{2+}, relaxation of phenylephrine-induced contractions was accompanied by inhibition of IP_3-mediated contractions, by NO-mediated re-uptake of Ca^{2+} to the SR, by repolarising the VSMC V_m and by inhibition of Ca^{2+} influx during the tonic contraction (Van Hove et al., 2009). To investigate whether the effects of NO on relaxation of VSMCs were voltage-dependent, the effects of NO were studied at different external K^+ concentrations or V_m of the VSMCs.

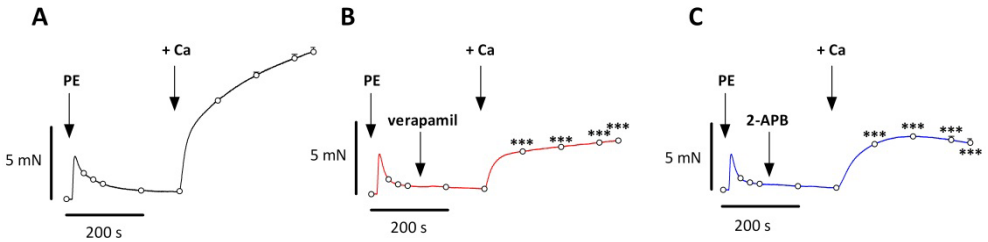

Figure 5. Phasic (transient) IP_3-mediated contraction by 2 μM (PE) in the absence of extracellular Ca^{2+}, followed by the tonic (SOCE) contraction upon re-addition of external Ca^{2+} (+3.5 mM Ca^{2+}) in control (A) and after addition of 10 μM verapamil (B) or 50 μM 2-APB (C) between the phasic and tonic contraction. Phasic force developed in B is due to non-selective cation Ca^{2+} influx and in C to L-type Ca^{2+} influx. The figure shows mean force traces with data±SEM at different time intervals; (n=4).

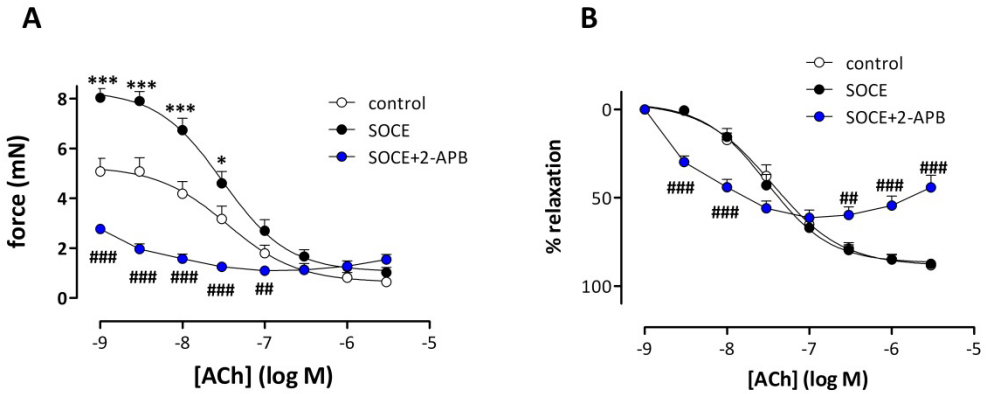

Figure 6. Absolute (A) and relative (B) ACh-induced relaxation of segments constricted with 2 μM phenylephrine in control conditions (white) and after eliciting SOCE by previously emptying the Ca^{2+} stores and re-adding external Ca^{2+} (black). Relaxation curves were fitted with sigmoidal concentration-response equations with variable slope. After inhibition of SOCE via non-selective cation channels with

50 μM 2-APB (blue), relaxation of phenylephrine-induced SOCE contraction by ACh, although very small, was completely different and compromised and could not be fitted with sigmoidal concentration-response equations (B). Data: mean±SEM; n=7; *, ***: P<0.05, 0.001 SOCE versus control; ##, ###: P<0.01, 0.001 2-APB versus SOCE.

5. Depolarization-induced contractions and NO

Aortic segments are unable to produce force upon depolarization with high K^+ in 0 mM Ca^{2+}. In the presence of extracellular Ca^{2+}, depolarization-induced contractions could be completely inhibited with CaBs, but were not affected by blocking the ryanodine receptor (15 μM ryanodine) or IP_3 receptor of the SR (50 μM 2-APB) (Peppiatt et al., 2003). These observations suggested that K^+-induced contractions of mouse aortic segments are solely supported by influx of Ca^{2+} via L-type Ca^{2+} channels. Figure 1 showed that ACh-induced relaxations of contractions produced by 20 mM extracellular K^+ (mild depolarization) were near complete and occurred with a sensitivity close to the ACh-sensitivity for relaxations of phenylephrine-induced contractions. However, for stronger depolarization, relaxation was severely compromised. The latter results suggest that relaxation of depolarization-induced contractions depended upon V_m of the VSMCs. V_m of the endothelial cells did not significantly contribute to the sensitivity to ACh because ACh-induced relaxations of phenylephrine-induced contractions at high extracellular K^+ in the presence of CaB were not attenuated (Van Hove et al., 2009). Why are relaxations of depolarized segments dependent on V_m of the VSMCs, i.e. complete for phenylephrine-induced contractions, which are also accompanied by depolarization of the segments, nearly complete for mild K^+-induced depolarization and severely attenuated for high K^+-induced depolarization? To solve this question we investigated the depolarization-induced contraction in more detail.

5.1. Depolarization-induced window contractions

Electrophysiological studies in isolated SMCs revealed the occurrence of a voltage range (window), in which L-type Ca^{2+} channels do not inactivate, leading to a "time-independent" influx of Ca^{2+} ions (Curtis & Scholfield, 2001; Fleischmann et al., 1994; Ganitkevich & Isenberg, 1990; Matsuda et al., 1990; Smirnov & Aaronson, 1992). This window influx of Ca^{2+} ions has been shown to lead to an increase of intracellular Ca^{2+} within the SMCs (Fleischmann et al., 1994), but has never been associated with the tonus of blood vessels. By clamping V_m of the endothelial and SMCs in aortic segments to depolarized potentials by elevating extracellular K^+, we were able to show a window contraction within the voltage range of overlap of activation and inactivation curves of the L-type Ca^{2+} channels (manuscript submitted, see also figure 8). In order to correlate the extracellular K^+ with V_m of the VSMCs of the aortic segments, V_m was measured with sharp glass intracellular microelectrodes (filled with 2 M KCl, tip resistances between 65 and 90 MΩ, HEKA EPC9 amplifier in the zero current-clamp mode). Deviation of measured V_m from the K^+ equilibrium potential (Nernstian V_K) was largest at physiological K^+ concentrations, indicating that in non-stimulated VSMCs other ions than K^+ contribute in setting the resting V_m (figure 7A). However, by adding levcromakalim, a drug that sets V_m to V_K by activating

ATP-dependent K^+ channels (Knot & Nelson, 1998; Weston et al., 2002), V_m of the VSMCs could be hyperpolarised to V_K. Indeed, when measured with intracellular microelectrodes, the resting V_m of VSMCs of aortic segments was -60.1±2.6 mV (n=8), which could be repolarized with levcromakalim to -84 mV.

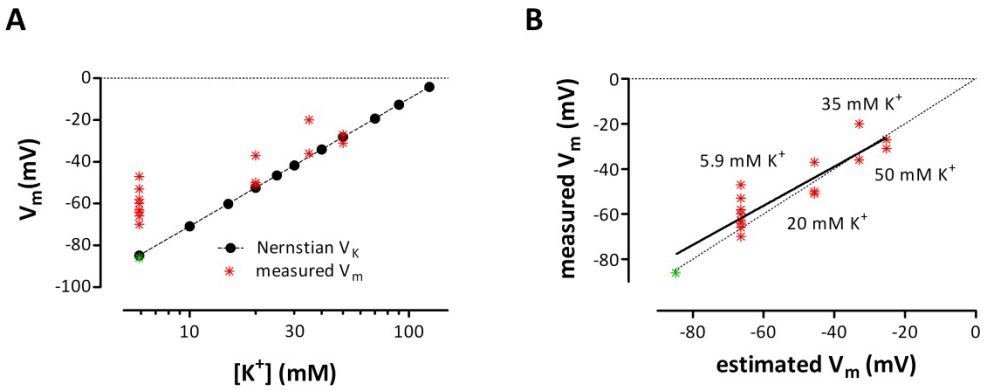

Figure 7. A: Relationship between extracellular K^+ and measured V_m (red asterisks) of mouse aortic VSMCs. Levcromakalim (green asterisk) caused hyperpolarization of V_m to V_K. The Nernstian relationship between V_K and extracellular K^+ is indicated by the black symbols and dotted line. B: Relationship between estimated and measured membrane potential (V_m) of mouse aortic VSMCs. Linear regression of the relationship between estimated and measured V_m (open circles, straight line) reveals slope of 0.90 (95% confidence interval 0.69-1.12), which was not significantly different from unity (dotted line) (R^2= 0.84). Full circle represents V_m in the presence of 200 nM levcromakalim at 5.9 mM K^+.

Taking into account the shift of the contraction curves at different K^+ in the presence of levcromakalim (see figure 8), V_m of the VSMCs evoked by increasing extracellular K^+ (V_{clamp}) could be estimated. V_{clamp} changed with K^+ concentration according to $V_{clamp} = 61*\log(([K^+]_o + 6)/[K^+]_i))$ with $[K^+]_o$ the extracellular K^+ concentration in mM, which is elevated by 6 mM as revealed by the shift induced by levcromakalim (figure 8), and $[K^+]_i$ the intracellular K^+ concentration (assumed to be 140 mM). Figure 7B shows that the relationship between the estimated and measured V_m was close to unity. This means that in the following graphs the K^+ axis could be replaced by a V_{clamp} axis. This is shown in figure 8, where the effects of levcromakalim on K^+-induced isometric contractions at different K^+ concentrations are considered. By adding levcromakalim, the aortic segments were all set to the same V_m, i.e. V_K.

Depolarization by elevated K^+ causes the isometric contraction to increase until maximal force of 100% was attained at 50 mM K^+. At higher K^+, force decreased again, leading to a bell-shape of the force-K^+ relationship, which agrees well with the bell-shaped voltage dependency of the L-type Ca^{2+} currents measured with voltage-clamp in single, isolated SMCs. The "steady-state" contractions observed at each K^+ concentration are window contractions, which are due to influx of Ca^{2+} via non-inactivating L-type Ca^{2+} channels. Differentiation of these contractions (%force/mM K^+ change) reveals a K^+-dependent contraction curve, which fits very well with the intracellular Ca^{2+} mobilized during the

depolarizing voltage clamp steps in single SMCs (Fleischmann et al., 1994). It is clear that levcromakalim, which causes repolarization of V_m from -60 to -80 mV, shifts the window contraction to higher extracellular K^+, indicating that in the presence of levcromakalim higher extracellular K^+ is needed to attain the same isometric contraction as in control. When contractions at different external K^+ concentrations were plotted as a function of V_{clamp}, contraction curves in the absence and presence of levcromakalim were identical (figure 8C, D). Hence, levcromakalim shifted the K^+-dependence of the isometric contraction, but not the voltage-dependence, suggesting that levcromakalim does not affect L-type Ca^{2+} channel gating properties. Results further suggest that at resting V_m of the VSMCs (-50 to -60 mV), V_{clamp} situates within the window voltage range, which results in continuous baseline Ca^{2+} influx and concomitant tonus via open L-type Ca^{2+} channels.

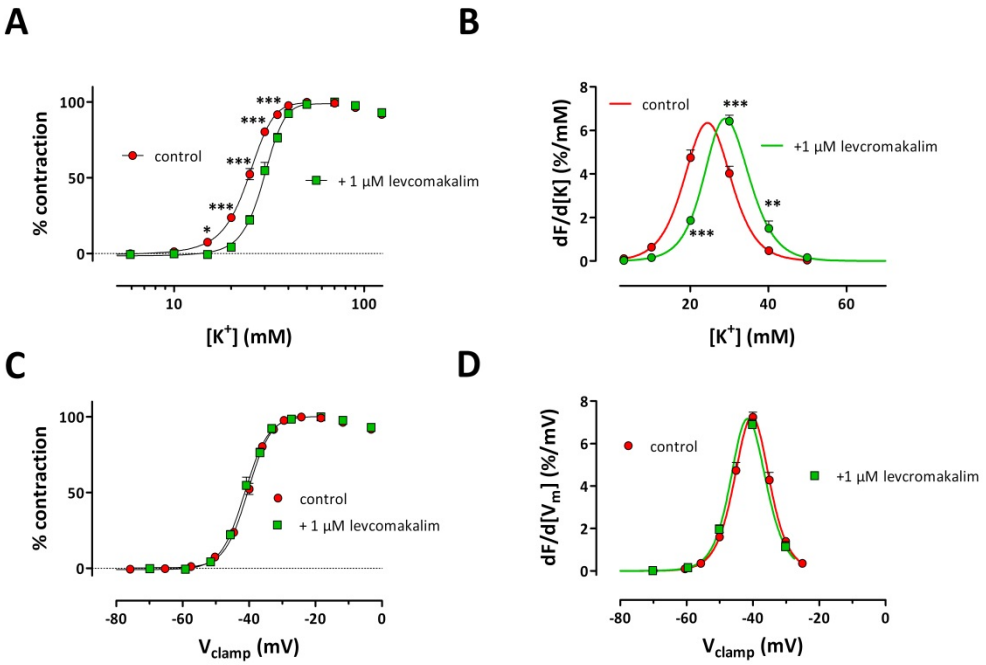

Figure 8. A and B: Effects of 1 µM levcromakalim on the K^+-dependence of the isometric contraction. Extracellular K^+ was increased from 2 mM to 124 mM in control (+300 µM LNAME/LNNA to inhibit eNOS) and in the presence of 1 µM levcromakalim to hyperpolarize the VSMCs to V_K. The fitted (sigmoidal concentration-response curves with variable slope) curves in A were differentiated in B to show K^+-dependence of the change of force development per mM change of K^+. Levcromakalim caused a significant rightward shift (± 6 mM) of the curves in A and B. C and D: Effects of 1 µM levcromakalim on the voltage-dependence of the isometric contraction. V_{clamp} was estimated as indicated in the text for control, i.e. absence of levcromakalim, and in the presence of levcromakalim, where V_{clamp} equals V_K. There was no shift of the voltage-dependence of the L-type Ca^{2+} channel-mediated contraction and the differentiated curves in D were equal. Data: mean±SEM; n=6; *, **, ***: P<0.05, 0.01, 0.001 levcromakalim versus control.

5.2. Depolarization-induced window contractions and NO

To investigate the effects of basal NO release on voltage-dependent L-type Ca^{2+} channel-mediated contractions, the contraction evoked by the increase of extracellular K^+ was measured before and after inhibition of eNOS with 300 μM LNAME/LNNA. NO has been described to activate voltage-gated K^+ channels, to hyperpolarize VSMCs and to decrease the intracellular Ca^{2+} concentration (Edwards et al., 2010; Quignard et al., 2000; Yuan et al., 1996). To compensate for the hyperpolarizing effects of NO or depolarizing effects of eNOS inhibition, 1 μM levcromakalim was added to set V_m of all the segments to V_K (figure 9). Inhibition of basal NO release shifted the contraction window to hyperpolarized potentials. A possible explanation is that S-nitrosylation of cysteine residues of the channel changes the voltage-dependence of the L-type Ca^{2+} channel-mediated contraction. Effects of NO and cGMP on L-type Ca^{2+} current have been described before. They might occur via an indirect mechanism through a NO-cGMP-PKG pathway and/or a direct mechanism mediated by S-nitrosylation (Almanza et al., 2007). The α1C-subunit of the L-type Ca^{2+} channel contains more than 10 cysteine residues that modulate channel gating and is constitutively S-nitrosylated in the mouse heart (Sun et al., 2006; Tamargo et al., 2010). According to this hypothesis, basal NO release should diminish Ca^{2+} influx via the L-type Ca^{2+} window at physiological V_m, leading to vasodilation. It will be interesting to test this hypothesis with intracellular VSMC Ca^{2+} measurements. Is intracellular Ca^{2+} decreasing upon addition of NO to segments pre-contracted with different K^+ (different V_{clamp})? Indirect evidence for the hypothesis is provided by the experiments of figure 1, where it was shown that the relaxing capacity of NO increased when external K^+ was decreased.

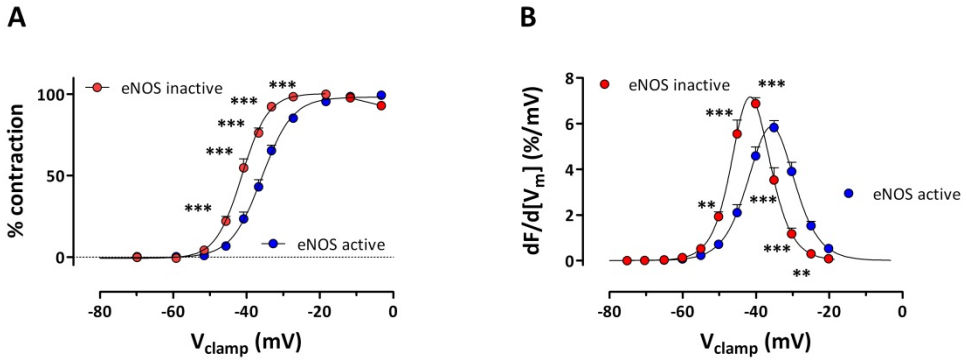

Figure 9. The contribution of basal NO release to window contractions. V_{clamp}-force curves for segments with active eNOS (blue, control segments) and segments with eNOS inhibited (red, 300 μM LNAME/LNNA combination) were constructed in the presence of 1 μM levcromakalim, which allowed to express force data as a function of V_{clamp} (= V_K). The fitted (sigmoidal concentration-response curves with variable slope) curves in A were differentiated in B to show the voltage-dependence of the change of force development per mV change of V_{clamp}. eNOS-inhibition caused a significant leftward shift of the eNOS active curves in A and B. Data: mean±SEM; n=6; **, ***: P<0.01, 0.001 eNOS inactive versus eNOS active.

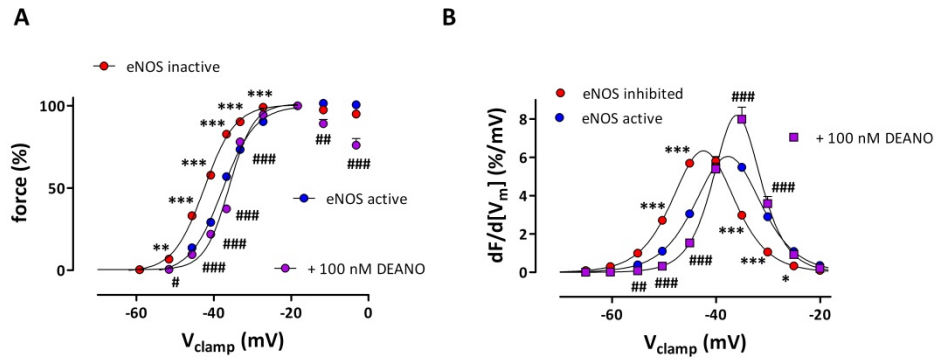

Figure 10. Effects of exogenous NO on contraction window in mouse aortic segments following re-polarization of V_m to V_K with 1 μM levcromakalim. eNOS was active (blue circles) or inhibited (red circles) and in this situation exogenous NO could be applied (100 nM DEANO, purple circles). The fitted (sigmoidal concentration-response curves with variable slope) curves in A were differentiated in B to show the voltage-dependence of the change of force development per mV change of V_{clamp}. Data: mean±SEM; n=4; *, **, ***: P<0.05, 0.01, 0.001 eNOS inactive versus eNOS active; #, ##, ###: P<0.05, 0.01, 0.001 +100 nM DEANO versus eNOS inactive.

The shift of the contraction window by eNOS inhibition could be completely reversed by adding exogenous NO (100 nM DEANO) (figure 10). The addition of exogenous NO to segments, in which eNOS activity was inhibited, caused a rightward (depolarising) shift of the voltage-dependency of contraction. Also in this situation, effects of eNOS inhibition or exogenous NO addition on V_m were avoided by performing the experiments in the presence of 1 μM levcromakalim. Results confirmed that NO altered the voltage-dependency of the L-type Ca^{2+} channel-mediated contraction, probably by direct effects of NO on the channel´s gating properties. It should be noted that for strong depolarization above -20 mV (90 and 124 mM K^+), addition of exogenous NO caused significant relaxation of the pre-constricted segments. Hence, the window contraction in the presence of NO is narrower than in the absence of NO (figure 10B). Whether these results can also be explained by NO-dependent changes of the voltage dependence of activation of the L-type Ca^{2+} channels needs further investigation.

The above data may provide an explanation for the absence of a decrease of intracellular VSMC Ca^{2+} with relaxation upon addition of NO to segments depolarized with 50 mM K^+, whereas similar experiments in phenylephrine-constricted segments displayed relaxation with an abrupt decrease of intracellular Ca^{2+} upon addition of NO (see figure 2). Firstly, depolarization with elevated K^+ did not empty the SR Ca^{2+} stores, and, hence, did not stimulate SOCE via NO-sensitive non-selective cation channels. Secondly, at 50 mM K^+ V_m of the VSMCs was clamped at depolarized potentials and NO cannot elicit hyperpolarisation of V_m. Thirdly, at 50 mM K^+, the window Ca^{2+} influx and concomitant contraction were maximal and addition of NO will only cause small relaxations, probably via effects on Ca^{2+}-sensitivity and not on intracellular Ca^{2+} concentrations.

6. NO efficacy and VSMC L-type Ca^{2+} channels along the thoracic aorta

Increased stiffness of elastic arteries represents an early risk factor for cardiovascular diseases (O'Rourke & Mancia, 1999) and, therefore, the assessment of mechanical properties of the aorta is important to understand the mechanisms of cardiovascular disease. It has been shown that in the aorta of C57Bl6 mice, the circumferential modulus is greatest (most rigid) near the diaphragm, and that about 85% of volume compliance is in the thoracic compared with abdominal aorta (Guo & Kassab, 2003). Because as well NO as CaBs have been described to de-stiffen large arteries (Fitch et al., 2006; Safar et al., 1989; Safar et al., 2011), we wondered whether NO release (basal and stimulated) and L-type Ca^{2+} channel activity differed along the length of the thoracic aorta.

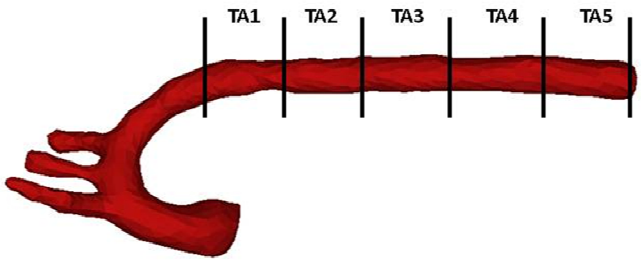

Figure 11. Dissection of the mouse thoracic aorta in five 2 mm wide segments. The mouse aorta was removed from the animal, stripped of adherent tissue and dissected systematically. Starting at the diaphragm, the ascending thoracic aorta was cut in segments of 2 mm width (TA5 up to TA1).

In this part of the chapter, we show some preliminary data on aortic segment differences with respect to NO and L-type Ca^{2+} channels. In order to test whether the release or efficacy of NO differs between different locations along the thoracic aorta of C57Bl6 mice, the aorta was divided into 5 segments (figure 11) and in each segment endogenous and exogenous NO efficacy was determined. Basal release of NO and its efficacy to counteract contraction was measured in each aortic segment by measuring isometric contractions to the α_1-adrenoceptor agonist phenylephrine before and after inhibition of eNOS with 300 μM LNAME/LNNA. The increase of force (Δ force) and the shift of $logEC_{50}$ (Δ logEC50) by eNOS inhibition are an index of the basal release of endogenous NO in each segment (figures 12A and B).

Although not significant, the effects of eNOS inhibition on phenylephrine-induced contractions were smaller in the atherosclerosis-resistant segments TA2, TA3 and TA4 as compared with the atherosclerosis-prone segments TA1 and TA5 (figure 12A). In accordance, inhibition of eNOS caused a significantly larger shift of the segment´s sensitivity to phenylephrine in the atherosclerosis-prone segment TA1 compared with the other segments (figure 12B). Results may point to a higher basal eNOS activity or release of basal NO in the atherosclerosis-prone segments TA1 and TA5. Subsequently, endogenous release of NO was evoked by adding increasing concentrations of ACh to segments pre-contracted with 1 μM phenylephrine. Figures 12C and D show maximal relaxation evoked by and sensitivity ($logEC_{50}$)

for ACh in each segment. Although TA1 seemed to have the highest NO efficacy without endothelial stimulation (basal NO, figures A and B), this atherosclerosis-prone segment caused only relaxations of about 65% and displayed the lowest sensitivity for ACh-induced relaxations. This was due to endothelial dysfunction because the effects of exogenous NO (DEANO) were not significantly different between the different aortic segments (figures 12 E and F). Results of these experiments show that endothelial function (basal and stimulated release of NO) may differ between atherosclerosis-prone and –resistant segments along the thoracic aorta of wild-type mice, which may have important consequences for the tonus and compliance of the thoracic aorta.

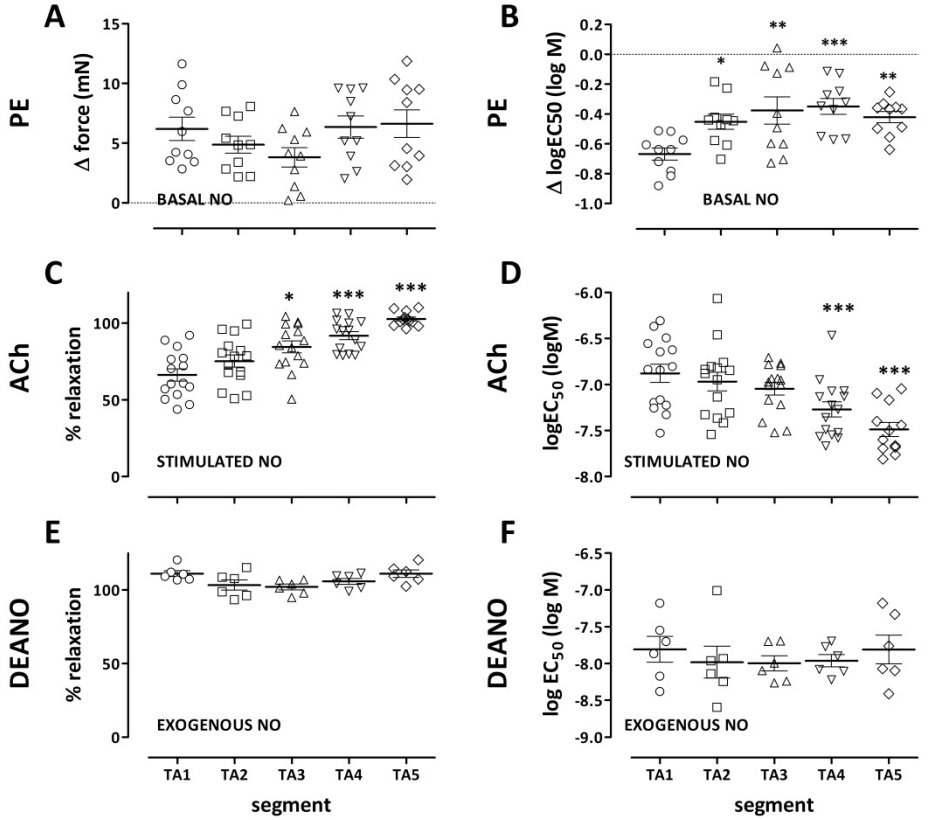

Figure 12. Basal and agonist-stimulated NO efficacy for different aortic segments. A and B show maximal increase of force development (Δforce) and the shift of the $logEC_{50}$ ($\Delta logEC_{50}$) for phenylephrine after inhibition of eNOS with the 300 μM LNAME/LNNA combination (measure of basal NO release). C and D show % relaxation and $logEC_{50}$ for ACh-induced relaxation of the contraction elicited with 1 μM phenylephrine (stimulated endogenous NO), hence in the absence of LNAME/LNNA. E and F show % relaxation and $logEC_{50}$ for DEANO-induced relaxation of the contraction elicited with 1 μM phenylephrine (exogenous NO) after inhibition of eNOS with 300 μM LNAME/LNNA. Data: mean ±SEM; n=6 or more; *, **, ***: P<0.05, 0.01, 0.001 versus TA1.

When the impact of ACh-stimulated eNOS activity on L-type Ca^{2+} channels was investigated further (see figure 6), but now in atherosclerosis-prone and -resistant segments, figures 13 A and C show that as well in the presence of external Ca^{2+} as after eliciting contraction by re-addition of Ca^{2+} to zero Ca^{2+} (SOCE contraction), relaxation in prone segments in comparison with resistant segments was attenuated. When SOCE via cation-selective channels was inhibited with 50 μM 2-APB, the SOCE contraction by phenylephrine was smaller in the resistant than in the prone segments (figure 13B, values at -9 logM ACh). Because this SOCE-contraction by phenylephrine is due to influx of Ca^{2+} via L-type Ca^{2+} channels only (see figure 5), this suggests that the L-type Ca^{2+} channel-mediated SOCE contraction in prone segments is larger than in resistant segments. This L-type Ca^{2+} channel-mediated contraction by phenylephrine in prone segments displayed attenuated relaxation to ACh (figure 13D), again pointing to the lower capacity of NO to relax contractions evoked by L-type Ca^{2+} influx.

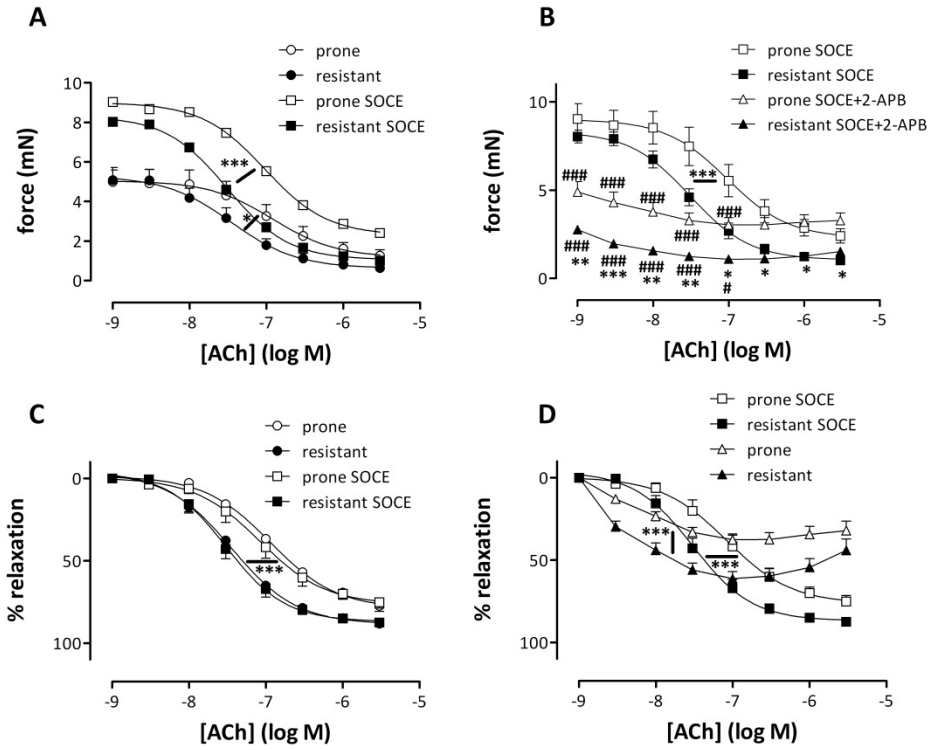

Figure 13. Absolute (mN, A, B) and relative (%, C, D) ACh-induced relaxation of atherosclerosis-prone (TA1,white symbols) and atherosclerosis-resistant (TA2/TA3, black symbols) segments constricted with 2 μM phenylephrine in the presence of extracellular Ca^{2+} (control conditions, circles) and after eliciting contraction by re-addition of external Ca^{2+} to zero Ca^{2+} (SOCE, squares). Relaxation curves were fitted with sigmoidal concentration-response equations with variable slope and significantly differed between prone and resistant segments. After inhibition of SOCE via non-selective cation channels with 50 μM 2-APB (triangles), the SOCE contraction, which is mediated through L-type Ca^{2+} influx only, was larger in prone than in resistant segments. Relaxation of these phenylephrine-induced SOCE contractions by

ACh were compromised more in prone than in resistant segments and could not be fitted with sigmoidal concentration-response equations (B). Data: mean±SEM; n=7; *, **, ***: P<0.05, 0.01, 0.001 prone versus resistant; #, ###: 2-APB versus SOCE.

7. Conclusions

The present chapter investigated the relaxing efficacy of NO for contractions induced by α_1-adrenoceptor stimulation with phenylephrine or by depolarization with elevated extracellular K^+ and confirmed previous observations that relaxation by NO is attenuated when the contraction was due to L-type Ca^{2+} influx (Van Hove et al., 2009). Contractions, which were initiated by Ca^{2+} release from the SR as with phenylephrine were very sensitive to endogenous or exogenous NO. Here, NO caused relaxation by inhibiting the IP_3-mediated contraction, by stimulating Ca^{2+} re-uptake to the SR via stimulation of SERCA, by inhibiting SOCE via cation channels and by reducing SOCE via L-type Ca^{2+} channels. Although phenylephrine has been described to cause depolarization of the VSMCs, V_m is not clamped at depolarized values and addition of NO is expected to cause hyperpolarization, thereby reducing Ca^{2+} influx via L-type Ca^{2+} channels. By clamping V_m to depolarized values with elevation of K^+, we were able to show contractions due to Ca^{2+} influx via L-type Ca^{2+} channels only and more specifically, to Ca^{2+} influx via non-inactivating Ca^{2+} channels (window contraction). This window contraction could be decreased by repolarizing V_m of VSMCs with levcromakalim (an opener of ATP-dependent K^+ channels) or by adding exogenous NO as long as the extracellular K^+ concentration was below 50 mM. Because NO also shifted the voltage-dependence of the window contraction in the presence of levcromakalim, it was hypothesized that NO, but not levcromakalim exerted a direct effect on the gating properties of the L-type Ca^{2+} channel. Although it has been described that NO affects L-type Ca^{2+} channels directly via S-nitrosylation (Almanza et al., 2007), an effect on the voltage-dependent contraction has not been directly demonstrated yet. Hence, it is hypothesized that in mouse aortic segments NO changed the voltage-dependence of the contraction mediated by L-type Ca^{2+} influx, probably via S-nitrosylation of the cysteine residues located in the gating part of the channel´s α1C-subunit.

An interplay between NO and L-type Ca^{2+} channels was also suggested by a number of other observations: a) When treated with the CaB, lacidipine, Western-type diet-evoked hypertension and atherosclerosis development in apoE-deficient mice was reduced, whereas endothelial function was preserved (Kyselovic et al., 2005), b) after partly inhibiting L-type Ca^{2+} influx induced by high K^+ with the CaB nifedipine, relaxation by exogenous NO was ameliorated (Van Hove et al., 2009) and c) $ApoE^{-/-}$ mice, which spontaneously develop atherosclerotic lesions at the age of 6 months when fed a normal diet, displayed altered Ca^{2+} homeostasis at the age of 4 months, hence, before development of plaques. In comparison with wild-type C57Bl6 mice, they showed higher baseline intracellular Ca^{2+} in the SMCs (Van Assche et al., 2007), lower baseline Ca^{2+} in endothelial cells and decreased basal but normal or even enhanced agonist-evoked NO release and efficacy (Fransen et al., 2008).

The present study might also provide an explanation for the unique features of the antihypertensive classes of CaBs with different chemical structure (phenylalkylamines such as verapamil,

benzothiazepines such as diltiazem and dihydropyridines such as nifedipine). They reduce blood pressure more effectively in hypertensive than in normotensive subjects (Leonetti et al., 1982) and they inhibit L-type Ca^{2+} influx more effectively in vascular tissue than in heart (Godfraind et al., 1984; Godfraind, 2005; Striessnig et al., 1998). Several attempts have been made to explain these unique features. In hypertension, there is an increase of reactivity to vasoconstrictors, which is not only due to a higher number of L-type Ca^{2+} channels (Godfraind, 2005; Pesic et al., 2004; Pratt et al., 2002), but also to depolarization of the resting potential of hypertensive VSMCs (Morel & Godfraind, 1994; Pesic et al., 2004). Depolarization leads to an increased proportion L-type Ca^{2+} channels in the inactivated state, which according to the "modulated receptor theory" may have higher affinity to CaBs than channels in the resting state (Bean et al., 1986; Godfraind, 2005; Morel & Godfraind, 1987). Cardiac muscle cells are hyperpolarized with respect to VSMC and hence less susceptible to block by CaBs. Another specific feature of L-type Ca^{2+} channels is that their population is not homogeneous because of the occurrence of alternatively spliced isoforms (Koch et al., 1990). Among the 55 known human L-type Ca^{2+} channel exons 19 undergo alternative splicing and display differences in tissue distribution, physiology, pharmacology and disease-related up- and/or down-regulation (Liao et al., 2005; Tang et al., 2007; Tiwari et al., 2006). Some of these isoforms were dominant in aorta (> 50%) and less abundant in heart (<5%). Moreover, the VSM-specific splice variant of the L-type Ca^{2+} channel displayed hyperpolarised window current at voltages where there is overlap between activation and inactivation curves and enhanced inhibition by nifedipine in comparison with the predominant cardiac isoform (Liao et al., 2007). The selective affinity of CaBs for the different L-type Ca^{2+} channel subpopulations may further contribute to the different susceptibility of VSMC or cardiac cells to CaBs. Because the L-type Ca^{2+} channel window in VSMCs may be responsible for "time-independent" baseline Ca^{2+} influx at normal resting or slightly depolarized membrane potentials (Fleischmann et al., 1994; Poburko et al., 2004), depolarization of the resting potential by hypertension not only favours the inactivated state of the L-type Ca^{2+} channel, but is also expected to increase L-type Ca^{2+} influx via the L-type Ca^{2+} channel window and to evoke inhibition by CaBs (Fleischmann et al., 1994).

Preliminary results of this chapter, finally, indicate that NO efficacy and L-type Ca^{2+} channel distribution may differ along the length of the thoracic aorta. Basal and stimulated eNOS activation or NO release occurred differently along the thoracic aorta. Close to the aortic arch, segments released more basal NO but less stimulated NO than segments close to the diaphragm. Similarly, L-type Ca^{2+} channel distribution and related window contraction were higher in atherosclerosis-prone than in -resistant segments. These preliminary data need to be further explored, but may have important consequences for the compliance of the different aortic segments and their susceptibility to the development of atherosclerosis.

Author details

Paul Fransen
Laboratory of Physiopharmacology, University of Antwerp, Wilrijk, Belgium

Cor E. Van Hove, Johanna van Langen and Hidde Bult
Laboratory of Pharmacology, University of Antwerp, Wilrijk, Belgium

8. References

Adapala, R. K.; Talasila, P. K.; Bratz, I. N.; Zhang, D. X.; Suzuki, M.; Meszaros, J. G.; & Thodeti, C. K. (2011) PKCalpha mediates acetylcholine-induced activation of TRPV4-dependent calcium influx in endothelial cells. *Am.J.Physiol Heart Circ.Physiol*,Vol.301, No.3, pp. H757-H765

Akata, T. (2007) Cellular and molecular mechanisms regulating vascular tone. Part 1: basic mechanisms controlling cytosolic Ca^{2+} concentration and the Ca^{2+}-dependent regulation of vascular tone. *J.Anesth.*,Vol.21, No.2, pp. 220-231

Al-Zobaidy, M. J.; Craig, J.; Brown, K.; Pettifor, G.; & Martin, W. (2011) Stimulus-specific blockade of nitric oxide-mediated dilatation by asymmetric dimethylarginine (ADMA) and monomethylarginine (L-NMMA) in rat aorta and carotid artery. *Eur.J.Pharmacol.*,Vol.673, No.1-3, pp. 78-84

Almanza, A.; Navarrete, F.; Vega, R.; & Soto, E. (2007) Modulation of voltage-gated Ca^{2+} current in vestibular hair cells by nitric oxide. *J.Neurophysiol.*,Vol.97, No.2, pp. 1188-1195

Bean, B. P.; Sturek, M.; Puga, A.; & Hermsmeyer, K. (1986) Calcium channels in muscle cells isolated from rat mesenteric arteries: modulation by dihydropyridine drugs. *Circ.Res.*,Vol.59, No.2, pp. 229-235

Bellien, J.; Favre, J.; Iacob, M.; Gao, J.; Thuillez, C.; Richard, V.; & Joannides, R. (2010) Arterial stiffness is regulated by nitric oxide and endothelium-derived hyperpolarizing factor during changes in blood flow in humans. *Hypertension*,Vol.55, No.3, pp. 674-680

Belz, G. G. (1995) Elastic properties and Windkessel function of the human aorta. *Cardiovasc.Drugs Ther.*,Vol.9, No.1, pp. 73-83

Bers, D. M. (2002) Cardiac excitation-contraction coupling. *Nature*,Vol.415, No.6868, pp. 198-205

Blatter, L. A. & Wier, W. G. (1994) Nitric oxide decreases $[Ca^{2+}]_i$ in vascular smooth muscle by inhibition of the calcium current. *Cell Calcium*,Vol.15, No.2, pp. 122-131

Bootman, M. D.; Collins, T. J.; Mackenzie, L.; Roderick, H. L.; Berridge, M. J.; & Peppiatt, C. M. (2002) 2-aminoethoxydiphenyl borate (2-APB) is a reliable blocker of store-operated Ca2+ entry but an inconsistent inhibitor of InsP3-induced Ca2+ release. *FASEB J.*,Vol.16, No.10, pp. 1145-1150

Cohen, R. A. & Adachi, T. (2006) Nitric-oxide-induced vasodilatation: regulation by physiologic s-glutathiolation and pathologic oxidation of the sarcoplasmic endoplasmic reticulum calcium ATPase. *Trends Cardiovasc.Med.*,Vol.16, No.4, pp. 109-114

Cohen, R. A.; Weisbrod, R. M.; Gericke, M.; Yaghoubi, M.; Bierl, C.; & Bolotina, V. M. (1999) Mechanism of nitric oxide-induced vasodilatation: refilling of intracellular stores by sarcoplasmic reticulum Ca^{2+} ATPase and inhibition of store-operated Ca^{2+} influx. *Circ.Res.*,Vol.84, No.2, pp. 210-219

Crauwels, H. M.; Van Hove, C. E.; Holvoet, P.; Herman, A. G.; & Bult, H. (2003) Plaque-associated endothelial dysfunction in apolipoprotein E-deficient mice on a regular diet. Effect of human apolipoprotein AI. *Cardiovasc.Res.*,Vol.59, No.1, pp. 189-199

Curtis, T. M. & Scholfield, C. N. (2001) Nifedipine blocks Ca^{2+} store refilling through a pathway not involving L-type Ca^{2+} channels in rabbit arteriolar smooth muscle. *J.Physiol*,Vol.532, No.Pt 3, pp. 609-623

Edwards, G.; Feletou, M.; & Weston, A. H. (2010) Endothelium-derived hyperpolarising factors and associated pathways: a synopsis. *Pflugers Arch.*,Vol.459, No.6, pp. 863-879

Essalihi, R.; Zandvliet, M. L.; Moreau, S.; Gilbert, L. A.; Bouvet, C.; Lenoel, C.; Nekka, F.; McKee, M. D.; & Moreau, P. (2007) Distinct effects of amlodipine treatment on vascular

elastocalcinosis and stiffness in a rat model of isolated systolic hypertension. *J.Hypertens.*,Vol.25, No.9, pp. 1879-1886

Fischmeister, R.; Castro, L.; Abi-Gerges, A.; Rochais, F.; & Vandecasteele, G. (2005) Species- and tissue-dependent effects of NO and cyclic GMP on cardiac ion channels. *Comp Biochem.Physiol A Mol.Integr.Physiol*,Vol.142, No.2, pp. 136-143

Fitch, R. M.; Rutledge, J. C.; Wang, Y. X.; Powers, A. F.; Tseng, J. L.; Clary, T.; & Rubanyi, G. M. (2006) Synergistic effect of angiotensin II and nitric oxide synthase inhibitor in increasing aortic stiffness in mice. *Am.J.Physiol Heart Circ.Physiol*,Vol.290, No.3, pp. H1190-H1198

Fleischmann, B. K.; Murray, R. K.; & Kotlikoff, M. I. (1994) Voltage window for sustained elevation of cytosolic calcium in smooth muscle cells. *Proc.Natl.Acad.Sci.U.S.A*,Vol.91, No.25, pp. 11914-11918

Fransen, P.; Katnik, C.; & Adams, D. J. (1998) ACh- and caffeine-induced Ca2+ mobilization and current activation in rabbit arterial endothelial cells. *Am.J.Physiol*,Vol.275, No.5 Pt 2, pp. H1748-H1758

Fransen, P.; Van Assche, T.; Guns, P. J.; Van Hove, C. E.; De Keulenaer, G. W.; Herman, A. G.; & Bult, H. (2008) Endothelial function in aorta segments of apolipoprotein E-deficient mice before development of atherosclerotic lesions. *Pflugers Arch.*,Vol.455, No.5, pp. 811-818

Frew, J. D.; Paisley, K.; & Martin, W. (1993) Selective inhibition of basal but not agonist-stimulated activity of nitric oxide in rat aorta by NG-monomethyl-L-arginine. *Br.J.Pharmacol.*,Vol.110, No.3, pp. 1003-1008

Ganitkevich, V. Y. & Isenberg, G. (1990) Contribution of two types of calcium channels to membrane conductance of single myocytes from guinea-pig coronary artery. *J.Physiol*,Vol.426, pp. 19-42

Godfraind, T. (2005) Antioxidant effects and the therapeutic mode of action of calcium channel blockers in hypertension and atherosclerosis. *Philos.Trans.R.Soc.Lond B Biol.Sci.*,Vol.360, No.1464, pp. 2259-2272

Godfraind, T.; Finet, M.; Lima, J. S.; & Miller, R. C. (1984) Contractile activity of human coronary arteries and human myocardium in vitro and their sensitivity to calcium entry blockade by nifedipine. *J.Pharmacol.Exp.Ther.*,Vol.230, No.2, pp. 514-518

Guo, X. & Kassab, G. S. (2003) Variation of mechanical properties along the length of the aorta in C57bl/6 mice. *Am.J.Physiol Heart Circ.Physiol*,Vol.285, No.6, pp. H2614-H2622

Isshiki, M.; Mutoh, A.; & Fujita, T. (2004) Subcortical Ca2+ waves sneaking under the plasma membrane in endothelial cells. *Circ.Res.*,Vol.95, No.3, pp. e11-e21

Isshiki, M.; Ying, Y. S.; Fujita, T.; & Anderson, R. G. (2002) A molecular sensor detects signal transduction from caveolae in living cells. *J.Biol.Chem.*,Vol.277, No.45, pp. 43389-43398

Karaki, H.; Ozaki, H.; Hori, M.; Mitsui-Saito, M.; Amano, K.; Harada, K.; Miyamoto, S.; Nakazawa, H.; Won, K. J.et al. (1997) Calcium movements, distribution, and functions in smooth muscle. *Pharmacol.Rev.*,Vol.49, No.2, pp. 157-230

Kauser, K.; da, C., V; Fitch, R.; Mallari, C.; & Rubanyi, G. M. (2000) Role of endogenous nitric oxide in progression of atherosclerosis in apolipoprotein E-deficient mice. *Am.J.Physiol Heart Circ.Physiol*,Vol.278, No.5, pp. H1679-H1685

Knot, H. J. & Nelson, M. T. (1998) Regulation of arterial diameter and wall [Ca^{2+}] in cerebral arteries of rat by membrane potential and intravascular pressure. *J.Physiol*,Vol.508 (Pt 1), pp. 199-209

Koch, W. J.; Ellinor, P. T.; & Schwartz, A. (1990) cDNA cloning of a dihydropyridine-sensitive calcium channel from rat aorta. Evidence for the existence of alternatively spliced forms. *J.Biol.Chem.*,Vol.265, No.29, pp. 17786-17791

Kyselovic, J.; Martinka, P.; Batova, Z.; Gazova, A.; & Godfraind, T. (2005) Calcium channel blocker inhibits Western-type diet-evoked atherosclerosis development in ApoE-deficient mice. *J.Pharmacol.Exp.Ther.*,Vol.315, No.1, pp. 320-328

Leonetti, G.; Cuspidi, C.; Sampieri, L.; Terzoli, L.; & Zanchetti, A. (1982) Comparison of cardiovascular, renal, and humoral effects of acute administration of two calcium channel blockers in normotensive and hypertensive subjects. *J.Cardiovasc.Pharmacol.*,Vol.4 Suppl 3, pp. S319-S324

Liao, P.; Yong, T. F.; Liang, M. C.; Yue, D. T.; & Soong, T. W. (2005) Splicing for alternative structures of $Ca_v1.2$ Ca^{2+} channels in cardiac and smooth muscles. *Cardiovasc.Res.*,Vol.68, No.2, pp. 197-203

Liao, P.; Yu, D.; Li, G.; Yong, T. F.; Soon, J. L.; Chua, Y. L.; & Soong, T. W. (2007) A smooth muscle $Ca_v1.2$ calcium channel splice variant underlies hyperpolarized window current and enhanced state-dependent inhibition by nifedipine. *J.Biol.Chem.*,Vol.282, No.48, pp. 35133-35142

Mancia, G.; De, B. G.; Dominiczak, A.; Cifkova, R.; Fagard, R.; Germano, G.; Grassi, G.; Heagerty, A. M.; Kjeldsen, S. E.et al. (2007) 2007 Guidelines for the Management of Arterial Hypertension: The Task Force for the Management of Arterial Hypertension of the European Society of Hypertension (ESH) and of the European Society of Cardiology (ESC). *J.Hypertens.*,Vol.25, No.6, pp. 1105-1187

Matsuda, J. J.; Volk, K. A.; & Shibata, E. F. (1990) Calcium currents in isolated rabbit coronary arterial smooth muscle myocytes. *J.Physiol*,Vol.427, pp. 657-680

Mian, K. B. & Martin, W. (1995) Differential sensitivity of basal and acetylcholine-stimulated activity of nitric oxide to destruction by superoxide anion in rat aorta. *Br.J.Pharmacol.*,Vol.115, No.6, pp. 993-1000

Mitchell, G. F. (1999) Pulse pressure, arterial compliance and cardiovascular morbidity and mortality. *Curr.Opin.Nephrol.Hypertens.*,Vol.8, No.3, pp. 335-342

Moosmang, S.; Schulla, V.; Welling, A.; Feil, R.; Feil, S.; Wegener, J. W.; Hofmann, F.; & Klugbauer, N. (2003) Dominant role of smooth muscle L-type calcium channel $Ca_v1.2$ for blood pressure regulation. *EMBO J.*,Vol.22, No.22, pp. 6027-6034

Morel, N. & Godfraind, T. (1987) Prolonged depolarization increases the pharmacological effect of dihydropyridines and their binding affinity for calcium channels of vascular smooth muscle. *J.Pharmacol.Exp.Ther.*,Vol.243, No.2, pp. 711-715

Morel, N. & Godfraind, T. (1994) Selective interaction of the calcium antagonist amlodipine with calcium channels in arteries of spontaneously hypertensive rats. *J.Cardiovasc.Pharmacol.*,Vol.24, No.4, pp. 524-533

Nakashima, Y.; Raines, E. W.; Plump, A. S.; Breslow, J. L.; & Ross, R. (1998) Upregulation of VCAM-1 and ICAM-1 at atherosclerosis-prone sites on the endothelium in the ApoE-deficient mouse. *Arterioscler.Thromb.Vasc.Biol.*,Vol.18, No.5, pp. 842-851

O'Rourke, M. F. & Mancia, G. (1999) Arterial stiffness. *J.Hypertens.*,Vol.17, No.1, pp. 1-4

Panza, J. A.; Casino, P. R.; Kilcoyne, C. M.; & Quyyumi, A. A. (1993) Role of endothelium-derived nitric oxide in the abnormal endothelium-dependent vascular relaxation of patients with essential hypertension. *Circulation*,Vol.87, No.5, pp. 1468-1474

Peppiatt, C. M.; Collins, T. J.; Mackenzie, L.; Conway, S. J.; Holmes, A. B.; Bootman, M. D.; Berridge, M. J.; Seo, J. T.; & Roderick, H. L. (2003) 2-Aminoethoxydiphenyl borate (2-APB) antagonises inositol 1,4,5-trisphosphate-induced calcium release, inhibits calcium pumps and has a use-dependent and slowly reversible action on store-operated calcium entry channels. *Cell Calcium*,Vol.34, No.1, pp. 97-108

Pesic, A.; Madden, J. A.; Pesic, M.; & Rusch, N. J. (2004) High blood pressure upregulates arterial L-type Ca^{2+} channels: is membrane depolarization the signal? *Circ.Res.*,Vol.94, No.10, pp. e97-104

Plane, F.; Wiley, K. E.; Jeremy, J. Y.; Cohen, R. A.; & Garland, C. J. (1998) Evidence that different mechanisms underlie smooth muscle relaxation to nitric oxide and nitric oxide donors in the rabbit isolated carotid artery. *Br.J.Pharmacol.*,Vol.123, No.7, pp. 1351-1358

Poburko, D.; Lhote, P.; Szado, T.; Behra, T.; Rahimian, R.; McManus, B.; van, B. C.; & Ruegg, U. T. (2004) Basal calcium entry in vascular smooth muscle. *Eur.J.Pharmacol.*,Vol.505, No.1-3, pp. 19-29

Pratt, P. F.; Bonnet, S.; Ludwig, L. M.; Bonnet, P.; & Rusch, N. J. (2002) Upregulation of L-type Ca^{2+} channels in mesenteric and skeletal arteries of SHR. *Hypertension*,Vol.40, No.2, pp. 214-219

Quignard, J.; Feletou, M.; Corriu, C.; Chataigneau, T.; Edwards, G.; Weston, A. H.; & Vanhoutte, P. M. (2000) 3-Morpholinosydnonimine (SIN-1) and K(+) channels in smooth muscle cells of the rabbit and guinea pig carotid arteries. *Eur.J.Pharmacol.*,Vol.399, No.1, pp. 9-16

Reddick, R. L.; Zhang, S. H.; & Maeda, N. (1994) Atherosclerosis in mice lacking apo E. Evaluation of lesional development and progression. *Arterioscler.Thromb.*,Vol.14, No.1, pp. 141-147

Rhee, S. W.; Stimers, J. R.; Wang, W.; & Pang, L. (2009) Vascular smooth muscle-specific knockdown of the noncardiac form of the L-type calcium channel by microRNA-based short hairpin RNA as a potential antihypertensive therapy. *J.Pharmacol.Exp.Ther.*,Vol.329, No.2, pp. 775-782

Richards, G. R.; Weston, A. H.; Burnham, M. P.; Feletou, M.; Vanhoutte, P. M.; & Edwards, G. (2001) Suppression of K(+)-induced hyperpolarization by phenylephrine in rat mesenteric artery: relevance to studies of endothelium-derived hyperpolarizing factor. *Br.J.Pharmacol.*,Vol.134, No.1, pp. 1-5

Safar, M. E.; Blacher, J.; & Jankowski, P. (2011) Arterial stiffness, pulse pressure, and cardiovascular disease-is it possible to break the vicious circle? *Atherosclerosis*,Vol.218, No.2, pp. 263-271

Safar, M. E.; Pannier, B.; Laurent, S.; & London, G. M. (1989) Calcium-entry blockers and arterial compliance in hypertension. *J.Cardiovasc.Pharmacol.*,Vol.14 Suppl 10, pp. S1-S6

Slama, M.; Safavian, A.; Tual, J. L.; Laurent, S.; & Safar, M. E. (1995) Effects of antihypertensive drugs on large artery compliance. *Neth.J.Med.*,Vol.47, No.4, pp. 162-168

Smirnov, S. V. & Aaronson, P. I. (1992) Ca^{2+} currents in single myocytes from human mesenteric arteries: evidence for a physiological role of L-type channels. *J.Physiol*,Vol.457, pp. 455-475

Striessnig, J.; Grabner, M.; Mitterdorfer, J.; Hering, S.; Sinnegger, M. J.; & Glossmann, H. (1998) Structural basis of drug binding to L Ca^{2+} channels. *Trends Pharmacol.Sci.*,Vol.19, No.3, pp. 108-115

Sun, J.; Picht, E.; Ginsburg, K. S.; Bers, D. M.; Steenbergen, C.; & Murphy, E. (2006) Hypercontractile female hearts exhibit increased S-nitrosylation of the L-type Ca^{2+} channel alpha1 subunit and reduced ischemia/reperfusion injury. *Circ.Res.*,Vol.98, No.3, pp. 403-411

Tamargo, J.; Caballero, R.; Gomez, R.; & Delpon, E. (2010) Cardiac electrophysiological effects of nitric oxide. *Cardiovasc.Res.*,Vol.87, No.4, pp. 593-600

Tang, Z. Z.; Hong, X.; Wang, J.; & Soong, T. W. (2007) Signature combinatorial splicing profiles of rat cardiac- and smooth-muscle $Ca_V1.2$ channels with distinct biophysical properties. *Cell Calcium*,Vol.41, No.5, pp. 417-428

Tiwari, S.; Zhang, Y.; Heller, J.; Abernethy, D. R.; & Soldatov, N. M. (2006) Atherosclerosis-related molecular alteration of the human $Ca_V1.2$ calcium channel alpha1C subunit. *Proc.Natl.Acad.Sci.U.S.A*,Vol.103, No.45, pp. 17024-17029

Tsai, E. J. & Kass, D. A. (2009) Cyclic GMP signaling in cardiovascular pathophysiology and therapeutics. *Pharmacol.Ther.*,Vol.122, No.3, pp. 216-238

Van Assche, T.; Fransen, P.; Guns, P. J.; Herman, A. G.; & Bult, H. (2007) Altered Ca^{2+} handling of smooth muscle cells in aorta of apolipoprotein E-deficient mice before development of atherosclerotic lesions. *Cell Calcium*,Vol.41, No.3, pp. 295-302

Van Assche, T.; Hendrickx, J.; Crauwels, H. M.; Guns, P. J.; Martinet, W.; Fransen, P.; Raes, M.; & Bult, H. (2011) Transcription profiles of aortic smooth muscle cells from atherosclerosis-prone and -resistant regions in young apolipoprotein E-deficient mice before plaque development. *J.Vasc.Res.*,Vol.48, No.1, pp. 31-42

Van Hove, C. E.; Van der Donckt, C.; Herman, A. G.; Bult, H.; & Fransen, P. (2009) Vasodilator efficacy of nitric oxide depends on mechanisms of intracellular calcium mobilization in mouse aortic smooth muscle cells. *Br.J.Pharmacol.*,Vol.158, No.3, pp. 920-930

Vanhoutte, P. M.; Shimokawa, H.; Tang, E. H.; & Feletou, M. (2009) Endothelial dysfunction and vascular disease. *Acta Physiol (Oxf)*,Vol.196, No.2, pp. 193-222

Vayssettes-Courchay, C.; Ragonnet, C.; Isabelle, M.; & Verbeuren, T. J. (2011) Aortic stiffness in vivo in hypertensive rat via echo-tracking: analysis of the pulsatile distension waveform. *Am.J.Physiol Heart Circ.Physiol*,Vol.301, No.2, pp. H382-H390

Westerhof, N.; Lankhaar, J. W.; & Westerhof, B. E. (2009) The arterial Windkessel. *Med.Biol.Eng Comput.*,Vol.47, No.2, pp. 131-141

Weston, A. H.; Richards, G. R.; Burnham, M. P.; Feletou, M.; Vanhoutte, P. M.; & Edwards, G. (2002) K^+-induced hyperpolarization in rat mesenteric artery: identification, localization and role of Na^+/K^+-ATPases. *Br.J.Pharmacol.*,Vol.136, No.6, pp. 918-926

White, D. G. & Martin, W. (1989) Differential control and calcium-dependence of production of endothelium-derived relaxing factor and prostacyclin by pig aortic endothelial cells. *Br.J.Pharmacol.*,Vol.97, No.3, pp. 683-690

Yuan, X. J.; Tod, M. L.; Rubin, L. J.; & Blaustein, M. P. (1996) NO hyperpolarizes pulmonary artery smooth muscle cells and decreases the intracellular Ca2+ concentration by activating voltage-gated K+ channels. *Proc.Natl.Acad.Sci.U.S.A*,Vol.93, No.19, pp. 10489-10494

Zhang, D. X.; Mendoza, S. A.; Bubolz, A. H.; Mizuno, A.; Ge, Z. D.; Li, R.; Warltier, D. C.; Suzuki, M.; & Gutterman, D. D. (2009) Transient receptor potential vanilloid type 4-deficient mice exhibit impaired endothelium-dependent relaxation induced by acetylcholine in vitro and in vivo. *Hypertension*,Vol.53, No.3, pp. 532-538

Zhou, Z. H.; Wang, J.; Xiao, H.; Chen, Z. J.; Wang, M.; Cheng, X.; & Liao, Y. H. (2008) A novel autoantibody in patients with primary hypertension: antibody against L-type Ca^{2+} channel. *Chin Med.J.(Engl.)*,Vol.121, No.16, pp. 1513-1517